NUMERICAL SIMULATION FOR EVACUATION PROCESS AGAINST TSUNAMI DISASTER AT TELUK BATIK IN MALAYSIA BY MULTI-AGENT DEM MODEL

Muhammad Salleh Abustan[1], Eiji Harada[2] and Hitoshi Gotoh[3]

[1]Graduate School of Engineering, Department of Civil and Earth Resource Engineering, Kyoto University, abustan_msa@yahoo.com.
[2] Department of Civil And Earth Resource Engineering, Kyoto University. harada@particle.kuciv.kyoto-u.ac.jp.
[3] Department of Civil And Earth Resource Engineering, Kyoto University. gotoh@particle.kuciv.kyoto-u.ac.jp.

The development of good individual behavior model is of significance to simulate the crowd behavior. Our research group has developed the Crowd Behavior Simulator for Disaster Evacuation (CBS-DE) based on the distinct element method (DEM). This DEM-base model for a tracking individual behavior has contributed to investigate an evacuation planning. Then the self-evasive action model has been introduced into the existing CBS-DE to simulate more realistic crowd behavior. With using this simulator, the pedestrian behavior, such as an avoidance of collision and an alignment between adjacent pedestrians are well reproduced in the contraflow. The contraflow may occurr in the evacuation process due to an unexpected situation. Hence, in the present study, the self-evasive action model is validated firstly by comparison with an observation, then numerical simulation for the evacuation process including contraflow is performed at Teluk Batik Beach in Malaysia. The effect of the self-evasive action model is shown in the context of the required time to complete evacuation.

***Key Words*:** *DEM, Self-evasive action Model, Evacuation analysis, Town planning.*

1. INTRODUCTION

The micro-simulator based on the distinct element method (DEM) has been applied to evacuation process by many researchers to simulate each individual behavior including contact force (e.g., Park et al., 2004; Kiyono et al., 1996, 1998). And each individual behavior model in the micro-simulator have been improved to simulate actual behavior. Our research group has developed the Crowd Behavior Simulator (CBS) based on the DEM. And problem for the evacuation process has been investigated computationally by using the Crowd Behavior Simulator for Disaster Evacuation (CBS-DE) (e.g., Gotoh et al., 2004, 2008). In recent year, the self-evasive model has been developed to improve the individual behavior by Gotoh et al. (2012). And the effect the self-evasive action model on the simulation results for the contraflow at crossing has been shown (Gotoh et al., 2012).

In this paper, the evacuation process against tsunami disaster at Teluk Batik in Malaysia has been carried out by using CBS-DE with self-evasive action model. And the significance of the description of individual behavior will be shown by comparison with CBS-DE simulation results with/without the self-evasive action model.

2. CROWED BEHAVIOR MODEL

(1) Fundamental equations

In this section, the CBS-DE with self-evasive action model (Gotoh et al., 2012) is outlined. The translational and rotational equations are employed for simulate each individual behavior as follows:

$$m_{hi}\dot{\boldsymbol{v}}_i = \mathbf{F}_{mi} + \mathbf{F}_{ci} + \mathbf{F}_{ei} \tag{1}$$

$$I_{hi}\dot{\boldsymbol{\omega}}_i = \mathbf{T}_i \tag{2}$$

where $\boldsymbol{v}_i$ = velocity of the person i, $\boldsymbol{\omega}_i$ = angular velocity of the person i, "$\cdot$" = time-derivative, $\dot{\boldsymbol{v}}_i$ = acceleration of the person i, $\dot{\boldsymbol{\omega}}_i$ = angular acceleration of the person i, $\mathbf{F}_{mi}$ = autonomous driving force of the person i, $\mathbf{F}_{ci}$ = interacting force acting on the person i, $\mathbf{F}_{ei}$ = self-evasive force showing either collision avoidance action or an alignment action, $\mathbf{T}_i$ = torque acting on the person i. In the present study, each individual person is simulated as a cylinder, thus, the mass and the moment of inertia of the person i, m_{hi} and I_{hi} respectively can be written as:

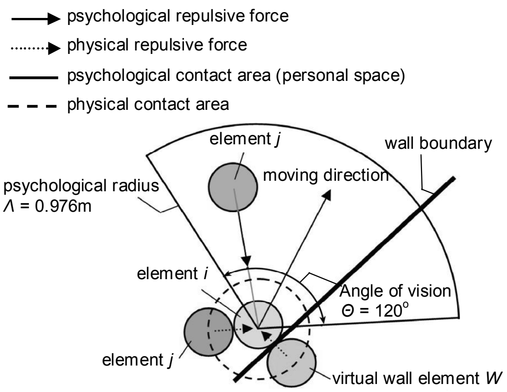

Fig. 1: Illustration of perception domain of each human.

$$m_{hi} = \varepsilon_{hi}\sigma_{hi}B_{hi}\frac{\pi d_{hi}^{2}}{4} \quad ; \quad I_{hi} = \varepsilon_{hi}\sigma_{hi}B_{hi}\frac{\pi d_{hi}^{4}}{32} \tag{3}$$

where σ_{hi} = density of the person i, B_{hi}= body height of the person i, d_{hi} = diameter of the person element i, ε_{hi} = correction coefficient concerning the volumetric difference between the cylinder element and the actual person.

(2) Interacting forces

Each individual person is controlled with the perception domain mobile territory as illustrated in Fig.1. Concerning to the physical repulsive force, the following conditions are given.

$$\left|\mathbf{r}_i - \mathbf{r}_j\right| \le \frac{d_{hi} + d_{hj}}{2} \quad ; \quad \left|\mathbf{r}_i - \mathbf{r}_W\right| \le \frac{d_{hi} + d_W}{2} \tag{4}$$

where $\mathbf{r}_i$ = positional vector of the person i, $\mathbf{r}_W$ = positional vector of the virtual wall element W, d_W= diameter of the virtual wall element W. While, the psychological repulsive force acts when two adjacent persons i and j satisfy the following condition:

$$\left|\mathbf{r}_i - \mathbf{r}_j\right| \le \Lambda \tag{5}$$

where Λ= psychological radius.

The total force acting on the person i is described as follows:

$$\mathbf{F}_{ci} = \mathbf{F}_{d(p/p)i} + \mathbf{F}_{d(W/p)i} + \mathbf{F}_{ps\_i} \tag{6}$$

$$\mathbf{F}_{d(p/p)i} = \sum_{j(\neq i)}\mathbf{f}_{ij} \quad ; \quad \mathbf{F}_{d(W/p)i} = \sum_{j(\neq i)}\mathbf{f}_{iW} \quad ; \quad \mathbf{F}_{ps\_i} = \sum_{j(\neq i)}\mathbf{f}_{ps\_ij} \tag{7}$$

$$\mathbf{T}_i = \frac{1}{2}\left\{\sum_{j(\neq i)}(\mathbf{r}_j - \mathbf{r}_i)\times\mathbf{f}_{ij} + \sum_{W}(\mathbf{r}_W - \mathbf{r}_i)\times\mathbf{f}_{iW}\right\} \tag{8}$$

where $\mathbf{F}_{d(p/p)i}$ = physical repulsive force acting on the person i, $\mathbf{F}_{d(W/p)i}$ = physical repulsive force between the virtual wall element W and the person i, $\mathbf{F}_{ps\_i}$= psychological repulsive force acting on the person i, $\mathbf{f}_{ij}$ = local physical repulsive force between the persons i and j, $\mathbf{f}_{iW}$ = local physical repulsive force between the person i and the virtual wall element W, $\mathbf{f}_{ps\_ij}$ = local psychological repulsive force between the persons i and j. These local repulsive forces $\mathbf{f}_{ij}$, $\mathbf{f}_{iW}$ and $\mathbf{f}_{ps\_ij}$ are given as follows:

$$\begin{aligned}\mathbf{f}_{com.} &= \left[\frac{\left(\mathbf{e}^n\right)^{pre} + k^n\Delta r^n\mathbf{n}}{\mathbf{e}^n} + \frac{c^n\Delta v^n\mathbf{n}}{\mathbf{d}^n}\right]_{com.} \\ &+ \left[\frac{\left(\mathbf{e}^t\right)^{pre} + k^t\Delta r^t\mathbf{t}}{\mathbf{e}^t} + \frac{c^t\Delta v^n\mathbf{t}}{\mathbf{d}^n}\right]_{com.} = \mathbf{f}^{\,n} + \mathbf{f}^{\,t}\end{aligned} \tag{9}$$

$$\mathbf{f}^{\,n} = \mathbf{e}^n + \mathbf{d}^n \quad ; \quad \mathbf{f}^{\,t} = \mathbf{e}^t + \mathbf{d}^t$$

$$\left.\begin{aligned} &\Delta r^n = [\mathbf{r}_{target} - \mathbf{r}_i]_{\Delta t}\cdot\mathbf{n} \quad ; \quad \Delta r^t = [\mathbf{r}_{target} - \mathbf{r}_i]_{\Delta t}\cdot\mathbf{t} \\ &d = |\,\mathbf{r}_i - \mathbf{r}_{target}| \\ &\mathbf{n} = (\mathbf{r}_i - \mathbf{r}_{target})/d = (n^1, n^2) \quad ; \quad \mathbf{t} = (-n^2, n^1) \\ &\Delta v^n = (\mathbf{v}_{target} - \mathbf{v}_i)\cdot\mathbf{n} \quad ; \quad \Delta v^t = (\mathbf{v}_{target} - \mathbf{v}_i)\cdot\mathbf{t} \end{aligned}\right\} \tag{10}$$

where $\mathbf{e}^n$ and $\mathbf{e}^t$ = component of the repulsive force due to the elastic springs, k^n and k^t = spring constants in the normal and the tangential directions, respectively, $\mathbf{d}^n$ and $\mathbf{d}^t$ = repulsive force due to the viscosity dashpots, c^n and c^t = dashpot constants in the normal and tangential directions, respectively, $\mathbf{f}^{\,n}$ and $\mathbf{f}^{\,t}$ = total repulsive force in the normal and tangential directions, respectively. The superscript "*pre*" indicates the previous numerical time step, $\mathbf{r}_{target}$ represents the positional vector of the target element. Subscript "*com.*" indicates ij, iW and ps_ij, and the corresponding the subscript "*target*" are the person j and the virtual wall element W.

(3) Autonomous driving force

We assume that the isolated person is accelerated up to the specific equilibrium velocity v_{limit} by the autonomous driving force $\mathbf{F}_{mi}$ as follows:

$$\mathbf{F}_{mi} = m_i\mathbf{a} \tag{14}$$

where $\mathbf{a}$ = acceleration vector. And the equilibrium velocity is subjected to number density of human. Therefore, the magnitude of the maximum equilibrium velocity v_{max} is given as follows:

$$v_{max} = v_{limit} - \gamma c_k \tag{15}$$

where γ is the proportional coefficient, v_{limit} = specific equilibrium velocity in an isolated walking condition, c_k = number density of persons inside the psychological perception area.

(4) Self-evasive force

In the present study, behavior of collision avoidance and an alignment are described by a

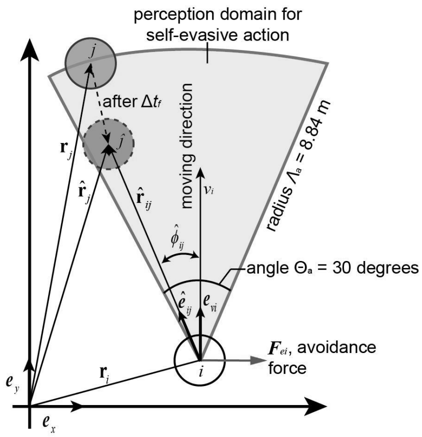

Fig. 2: Perception domain for self-evasive action.

single model introducing the self-evasive force, since both actions are closely related in each other. The self-evasive force is estimated by referring the predicted position of surrounding pedestrians after Δt_f seconds as shown in Fig. 2. Based on observation by Tatabe et al. (1994), the turning angle to avoid the static obstacle is $\Theta_a = \pm 15^{\circ}$ and radius of the perception domain for self-evasive action is Λ_a = 8.84m. The self-evasive force is described as follows:

$$\mathbf{F}_{ei} = \begin{cases} m_i \sum_{j(\neq i)}^{N_k} \kappa \dfrac{(\mathbf{v}_i - \mathbf{v}_j)\cdot \mathbf{e}_{vi}}{\Delta t_f} (\hat{\mathbf{e}}_{ij} \times \mathbf{e}_{vi}) \times \mathbf{e}_{vi} & when\, \hat{\mathbf{e}}_{ij} \times \mathbf{e}_{vi} \neq \mathbf{0} \\ m_i \sum_{j(\neq i)}^{N_k} \kappa \dfrac{(\mathbf{v}_i - \mathbf{v}_j)\cdot \mathbf{e}_{vi}}{\Delta t_f} (\mathbf{e}_x \times \mathbf{e}_y) \times \mathbf{e}_{vi} & when\, \hat{\mathbf{e}}_{ij} \times \mathbf{e}_{vi} \neq \mathbf{0} \end{cases} \tag{16}$$

$$\kappa = \alpha \frac{\cos \hat{\phi}_{ij}}{|\hat{\mathbf{r}}_{ij}| / r_v}; \quad \cos \hat{\phi}_{ij} = \mathbf{e}_{vi} \cdot \hat{\mathbf{e}}_{ij} \tag{17}$$

$$\hat{\mathbf{r}}_{ji} = \hat{\mathbf{r}}_j - \mathbf{r}_i; \quad \hat{\mathbf{r}}_j = \mathbf{r}_j + \mathbf{v}_j \Delta t_f \tag{18}$$

where N_k = total number of pedestrian in the perception domain of self-evasive action, Δt_f = time for the self-evasive action, $\mathbf{e}_{vi}$ = unit vector in the $\mathbf{v}_i$ direction, $\hat{\mathbf{e}}_{ij}$ = unit vector in the $\hat{\mathbf{r}}_{ji}$ direction, $\mathbf{e}_x$ and $\mathbf{e}_y$ = unit vector in the x- and y-axis, respectively, α = proportional coefficient, $\hat{\mathbf{r}}_j$ = predicted positional vector of the pedestrian j after Δt_f s. Eq. (16) indicated that in the case of approaching relative traveling velocity between the pedestrians i and j, the avoidance force acts on the pedestrians i, meanwhile, the alignment force acts on the pedestrian i in the case of depending relative velocity between the pedestrians i and j. As for the singularity treatment, when the unit vector $\hat{\mathbf{e}}_{ij}$ equals

Table 1: Setup procedure of model constants between persons.

		physical repulsive force, **ij**	psychological repulsive force, **ps ij**
spring	k^n	$k^n = 1.26\times10^4$ N/m	$k^n = \dfrac{Ma}{\Lambda - \dfrac{d_h}{2}}$
	k^t	$k^n \times 0.05$	$k^n \times 0.05$
dashpot	c^n	$2(Mk^n)^{1/2}$	$2(Mk^n)^{1/2}$
	c^t	$2(0.05Mk^n)^{1/2}$	$2(0.05Mk^n)^{1/2}$

with the unit vector $\mathbf{e}_{vi}$ the avoidance force $\mathbf{F}_{ei}$ acts on pedestrian i in the right direction perpendicular to the travelling direction of the pedestrian i.

(5) Model constants

Setup procedure of model constants shown in Table 1 is employed with referring Kiyono et al. (1998). According to this procedure, all of constants for spring and dashpot are determined automatically by giving a normal spring constant, k^n. The physical normal spring constant k^n (=1.26×10^4 N/m), which was measured with compressing actual human body, is used. Otherwise, the psychological normal spring constant k^n between persons is determined by setting autonomous driving force so as to be equal to the normal component of the psychological force under the minimum psychological distance between pedestrians. And, the relation between spring and dashpot constants is set to satisfy the critical damping condition of the Voigt model in a single degree of freedom. And the tangential spring constant is given as 0.05 times as much as the normal spring constant.

3. MODEL VERIFICATION

(1) Observation and simulation condition

To validate the CBS-DE with self evasive action model, simulation results for the crossing behavior are compared with the observation. Fig 3(a) shows the observation area, the scale of which is 12.6 m in length and 4.6 m in width. The crossing behavior has been filmed and the trajectories every 0.5 seconds of pedestrian behavior have been extracted by the image analysis. In addition, the statistical data for equilibrium walking velocities by ages have also been derived. And simulations with using these derived distributions of velocities have been implemented. Simulations have been performed under the same condition.

(2) Effect of self-evasive action model

To validate the self-evasive action model, simulations of contraflow of pedestrian with

Table 2: Detail population in Teluk Batik Beach

Category	Sex	Age	People	Ratio [%]	Velocity [m/s]
1	Male	10-39	484	32.01	**1.38**
2	Female	10-39	499	33.00	**1.20**
3	Male	40-69	161	10.65	**1.14**
4	Female	40-69	194	12.83	**1.04**
5	Male	>70	0	0.00	**0.99**
6	Female	>70	0	0.00	**0.89**
7	Child	5-9	174	11.51	**1.06**
		Total	**1512**	**100 %**	

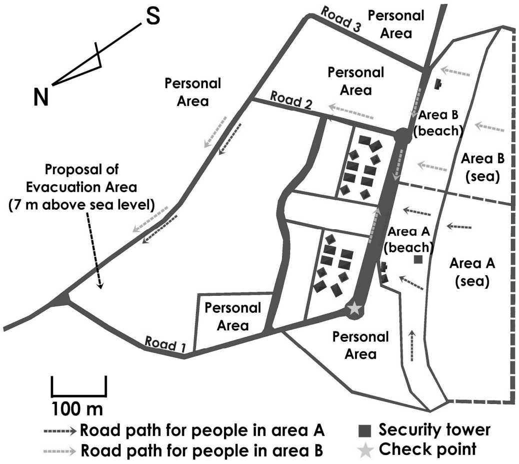

Fig. 4: Computational domain and evacuation route

model-1 and model-2 are compared with the observation; model-1 is the simulation by using the CBS-DE while model-2 is the simulation by using the CBS-DE with self-evasive action model. Fig. 3 (b) shows the typical snapshot of whole pedestrian behavior of model-1, model-2 and observation results. From the snapshot, at the time t =11.0 s, the alignment is reproduced in the model-2, while such alignment is not formed in the result with model-1. In comparison with the observation, we can find higher reproducibility of the model-2 to the actual contraflow than the model-1. Therefore the effect of the self-evasive action model is confirmed.

4. EVACUATION PROCESS

Teluk Batik Beach area is a place where receives thousands of visitors, located at west coast of the state of Perak in Malaysia. Hence a suitable planning, which assures safety of people during emergency or disaster even when an unusual behavior of the crowd occurs, is required. According to the field surveys, the culmination distribution of population is observed as shown in Table 2. In the simulation people are randomly arranged at the initial condition.

a)

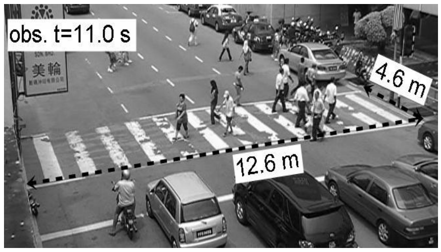

b)

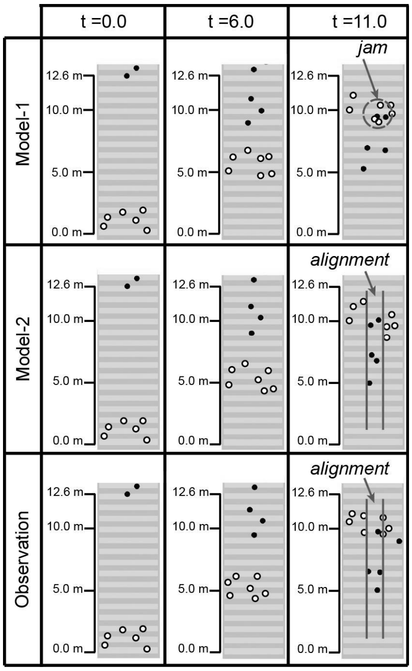

Fig. 3: (a) Pedestrian behavior at the crossing in Malaysia, (b) Snapshots of contra-flow of model-1, model-2 and observation.

(1) Simulation setup

Fig. 4 shows the setup of evacuation route for the simulation of evacuation process against tsunami. The complete evacuation is assumed that all people safely move to designated evacuation place. Although peoples in the area A typically use the road 1 as a convenience road to access the beach area, we specify the road 2 as evacuation road to consider the severe evacuation situation. Thus, we have set the following condition: the people in area B does not notice that the road 1 is closed till they arrive at check point area and return back to the road 2 to continue the evacuation process. We also assume that information about tsunami warning spreads at the security tower with the speed of 1.5 m/s. And the people start their movement after receiving the tsunami warning.

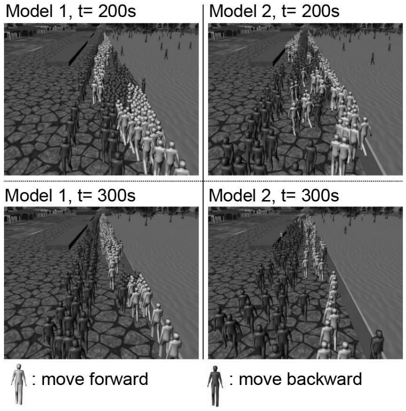

Fig. 5: CG-snapshot of bidirectional crowd flow: model-1 (left); model-2 (right).

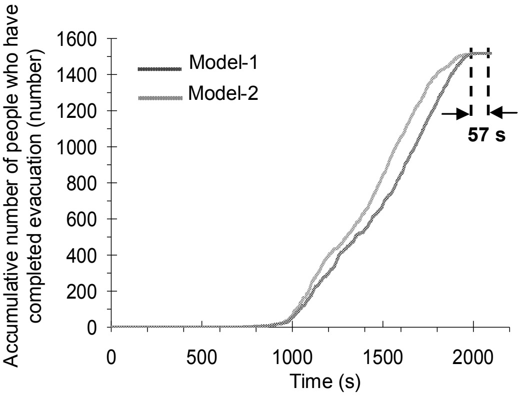

Fig 6: Time series of the accumulative number of people who have completed evacuation of model-1 and model-2 respectively.

(2) Evacuation simulation

To show the effect of introducing the self-evasive model on the crowded evacuation behavior, simulations with model-1 and model-2 have been performed. Fig. 5 shows the snapshot for evacuation process. The significant jam with crowd can be found in the snapshot of the model-1 at the time t = 200 s. And this kind of jam is often observed as shown in the snapshot of the model-1 at the t =300 s. These jams with crowd are obviously considered incomprehensible. On the other hand, such severe jams are not found in the model-2. And smooth contra-flow formed by bidirectional crowd flow is simulated. Fig. 6 shows the time series of the accumulative number of people who have completed evacuation. The fully completed time of evacuation in the model-2 decrease by 57 second in comparison to the model-1 as shown in Fig. 6. This fact supports the effect of self-evasive action model. Significance of the development of appropriate crowd behavior model to the implementation of this kind of evacuation simulation is inferred.

5. CONCLUSION

The statistical data related to the equilibrium walking velocity by ages for Malaysian have been analyzed by using the video image taken at crossing in Malaysia. Then the validity of the CBS-DE with self-evasive action model has been shown by comparison with observed results of the contraflow at crossing. And the evacuation process against tsunami disaster at Teluk Batik beach in Malaysia has been performed by using the CBS-DE with/without the self-evasive action model. The significant effect of the introduction of self-evasive action model have been found in the simulation results.

REFERENCES

Gotoh, H., Harada, E., Kubo, Y., and Sakai, T. (2004): Particle-System Model of the behavior of Crowd in Tsunami Flood Refuge, *Annual Jour. Of Coastal Engineering, JSCE,* Vol.51, pp.1261-1265 (in Japanase).

Gotoh, H., Harada, E., and Ohniwa, K. (2009): Numerical Simulation of Coastal Town Planning against Tsunami by DEM-base Human Behavior Simulator, *Proceeding of the Nineteenth (2009) International Offshore and Polar Engineering Conference,* Osaka, Japan, pp.1248-1252.

Gotoh, H., Harada, E., and Andoh, E. (2012): Simulation of pedestrian contra-flow by multi-agent DEM model with self-evasive action model, *Safety Science*, 50 (2012) pp.326-332.

Kiyono, J., Miura, F., and Takimoto, K. (1996): Simulation of emergency evacuation behaviour during disaster by using distinct element method, *Journal of structural mechanics and earthquake engineering, JSCE,* 591(I-43), pp.365-378 (in Japanese).

Kiyono, J., Miura, F., Yagi, H., (1998): Simulation of evacuation behavior in a disaster by distinct element method, *Journal of structural mechanics and earthquake engineering, JSCE,* 591(I-43), pp.365-378 (in Japanese).

Park, J., Lee, D., Kim, H., and Yang, Y. (2004): Development of evacuation model for human safety in maritime casualty. *Ocean Engineering* 31, pp.1537-1547.

Tatebe, K., Tsujimoto, M., Shida, K., (1994): Method for judging the beginning point of avoiding behavior, and avoidance distance between pedestrian and standing obstacle. *Journal of Architecture, Planning and Environment Engineering AIJ* 465, 95-104 (In Japanese).

(Received Jun 15, 2012)